

A search for radio emission from Galactic supersoft X-ray sources

R. N. Ogle^{1,2}, S. Chaty², M. Crocker³, S. P. S. Eyres⁴, M. A. Kenworthy⁵,
A. M. S. Richards³, L. F. Rodríguez⁶ and A. M. Stirling⁴

¹ Department of Physics, Keele University, Staordshire ST5 5BG

² Department of Physics and Astronomy, The Open University, Walton Hall, Milton Keynes, Buckinghamshire MK7 6AA

³ University of Manchester, Jodrell Bank Observatory, Macclesfield, Cheshire SK11 9DL

⁴ CFA, University of Central Lancashire, Preston PR1 2HE

⁵ Steward Observatory, 933 North Cherry Avenue, Tucson, AZ 85721, USA

⁶ Instituto de Astronomía, UNAM, Campus Morelia, Apdo. Postal 3-72, Morelia, Michoacán 58089, Mexico

19 March 2024

ABSTRACT

We have made a deep search for radio emission from all the northern hemisphere supersoft X-ray sources using the VLA and MERLIN telescopes, at 5 and 8.4 GHz. Three previously undetected sources: T Pyx, V1974 Cygni and RX J0019.8+2156 were imaged in quiescence using the VLA in order to search for any persistent emission. No radio emission was detected in any of the VLA fields down to a typical 11 RM S noise of 20 Jy beam⁻¹, however, 17 new point sources were detected in the fields with 5 GHz fluxes between 100 and 1500 Jy giving an average 100 Jy-source density of 200 per square degree, comparable to what was found in the MERLIN HDF survey. The persistent source AG Draconis was observed by MERLIN to provide a confirmation of previous VLA observations and to investigate the source at a higher resolution. The core is resolved at the milliarcsec scale into two components which have a combined flux of 1 mJy. It is possible that we are detecting nebulousity which is becoming resolved out by the higher MERLIN resolution. We have investigated possible causes of radio emission from a wind environment, both directly from the secondary star, and also as a consequence of the high X-ray luminosity from the white dwarf. There is an order of magnitude discrepancy between observed and modelled values which can be explained by the uncertainty in fundamental quantities within these systems.

Key words: binaries: general { novae, cataclysmic variables { white dwarfs { Radio continuum : stars { X-rays: stars

1 INTRODUCTION

Supersoft sources are a separate class of X-ray objects. The most popular explanation of these sources is a white dwarf & sub-giant companion with a high accretion rate, 100{1000 times greater than in cataclysmic variables (van den Heuvel et al. 1992). The large accretion rate creates steady hydrogen burning on the white dwarf surface causing X-ray emission.

Supersoft sources are difficult to detect in the Galaxy as the high column density in the Galactic plane absorbs most of the soft X-ray radiation. Consequently there have been many more detections at high galactic latitudes such as in the LMC, SMC and M31. As of 1999 (Greiner 2000), there were 57 supersoft sources: 10 in the Galaxy, 4 in the

SMC, 8 in the LMC and 34 in M31 and 1 in NGC 55. Consequently, even though sources in the LMC and SMC are further away, they have been studied in greater detail due to their larger numbers. For example, in 1997 Fender, Southwell & Tzioumis (1998) searched for radio emission from non-Galactic supersoft sources despite them being prohibitively further away than their Galactic counterparts.

Of the persistent super-soft sources, three have been reported to have outflows, detected by emission lines in their optical and infrared spectra. What is the makeup of these sources, and are they the link between the low velocity jets seen in star-forming systems, and the superluminal jets seen in the microquasars?

² E-mail: mo@astro.keele.ac.uk

1.1 Sources without outflow

Three supersoft sources have been observed with weak Doppler-shifted optical emission lines. The first object to be detected was RX J0513.9-6951, an LMC object which was discovered during an outburst in 1990 (Schaeidt et al. 1993), and optically identified by Pakul et al. (1993) and Cowley et al. (1993). This source has persistent optical emission with dips in the lightcurve every 100(200 days (Southwell et al. 1996). The evidence for jets in this source comes from strong He II, H and H lines with Doppler-shifted components at 4000 km s⁻¹ (Southwell et al. 1996). These lines are still observed during an optical dip, but with a reduced equivalent width, implying a reduction in the accretion rate.

The second supersoft jet source to be detected was RX J0019.8+2156 (Beuermann et al. 1995), a Galactic object at 2 kpc consisting of a 1 M WD and a 1.5 M donor star (Becker et al. 1998). The optical spectrum shows strong He I emission and P Cygni absorption in the Balmer lines. This source displays slower red and blue-shifted lines with velocities of 815 km s⁻¹, but these lines have a high FWHM of 400 km s⁻¹ (Tomov et al. 1998). Quaintrell & Fender (1998) have also found these features in infrared spectra. Becker et al. (1998) conclude that the jets in this system come from an inclined cone of material blown off from an accretion disc.

The third, and last, supersoft source to be discovered with an outflow is the Galactic source RX J0925.7-4758. This was observed by Motch (1998) over two nights in 1997. Spectra showed prominent H blue and red-shifted lines with a velocity of 5800 km s⁻¹. Motch (1998) modelled the emission from a cone with a large opening angle, at low inclination, similar to RX J0019+2156.

The only radio detection of a supersoft source was that of the symbiotic star AG Draconis (Torbett & Campbell 1987; Seaquist et al. 1993). Observations with the VLA showed two unresolved components separated by 1'', at fluxes of 200 and 400 Jy, shown in figure 1(a). These authors conclude that the emission is from optically thick thermal free-free emission, based on the majority of symbiotic systems. However, we cannot rule out optically thick emission in this paper.

2 OBSERVATIONS

Of the ten Galactic supersoft sources, four were observed by the VLA. These are RX J0019.8+2156, T Pyx, AG Draconis and V1974 Cygni. Three of these sources were observed with the VLA with the exception of AG Dra which was observed using MERLIN for the purpose of resolving any detail.

As we were primarily concerned with initial detections of point sources, a standard continuum setup was used for both the VLA and MERLIN observations. For the VLA we used a 100 MHz bandwidth split into two channels, and for MERLIN we used a 15 MHz bandwidth split into 15 channels. Individual channels were retained in order to reduce the amount of bandwidth smearing of sources offset from the phase-centre.

2.1 T Pyxis

T Pyx is a recurrent nova first discovered by Leavitt (1914) at a distance of 1.5 kpc (Shara 1997; Margon & Deutsch 1998). An arcsecond size optical nebula around the source, which shows a large amount of clumpy material on sub-arcsec scales, was detected from this object (Williams 1982; Duerbeck & Sitter 1987). This clumpy material would provide a rich medium for interaction with an outflow, such as the 1100(1400 km s⁻¹ jets reported by Shahbaz et al. (1997) (however, this outflow probably originates in the surrounding nebular, and not in jets, see O'Brien & Cohen (1998) and Margon & Deutsch (1998)).

Observations were taken using the VLA in CnB configuration on 2000 March 3, 0415-0615 UT at 8.4 GHz and in Dn configuration on 2000 September 26 & 28, 1600-1710 & 1400-1630 UT respectively. Data were calibrated using the standard flux calibrator 3C 147, and phase calibrator PKS J0921-2618. No emission was observed from either the source, or any of the 7 surrounding sources from the SIMBAD database. We can put a 1 RM S upper limit of 22 Jy beam⁻¹ at 4.8 GHz, and 19 Jy beam⁻¹ at 8.4 GHz.

An observing log, together with beam sizes, RM S noise and source details for all sources is given in table 1.

2.2 V1974 Cygni (Nova Cygni 1992)

V1974 Cygni was extensively studied at all wavelengths following an outburst in 1992. Complementary VLA and MERLIN images show that the source initially flared then decayed, as a shell from the outburst expanded (Hjellming 1992; Eyres et al. 1996). They concluded that the emission from the nova was thermal and initially optically thick, then gradually became optically thin. This is expected from an expanding shell of material.

This source was observed by the VLA in CnB configuration on 2000 March 09 & 10 at 1500-1600 and 1330-1430 UT respectively at 8.4 GHz and in Dn configuration on 2000 June 27 at 0800-0945 UT at 4.8 GHz. Data were calibrated using the standard flux calibrator 3C 286 and phase-referenced using Ohio W 538. No emission was detected from Nova Cygni 1992. We can put a 1 RM S upper limit to any emission of 24.6 Jy beam⁻¹ at 4.8 GHz, and 19.8 Jy beam⁻¹ at 8.4 GHz.

2.3 RX J0019.8+2156 (QR Andromedae)

RX J0019.8+2156 was observed by the VLA in CnB configuration on 2000 March 11 at 1810-2050 UT at 8.4 GHz and in Dn configuration on 2000 June 27 at 1300-1530 UT at 4.8 GHz. The flux calibrator used was 3C 48 and the data were phase referenced using PKS J0010+1724. No emission was detected from RX J0019.8+2156. We can therefore put a 1 RM S upper limit to any emission of 22.7 Jy beam⁻¹ at 4.8 GHz, and 19.8 Jy beam⁻¹ at 8.4 GHz.

2.4 AG Draconis

To confirm the previous VLA detection, shown in figure 1(a), we observed AG Dra on 2000 March 18, 25 & 26 at 1010(1130, 0630(2140 and 0510(2250 UT respectively with MERLIN. Due to the superior resolving power of MERLIN

Table 1. Observation log and source details. Please note that the MERLIN observations are only at 5 GHz and the two fluxes presented are for two components in the image.

T Pyx		
Band	4.8 GHz (C)	8.4 GHz (X)
Telescope	VLA D	VLA CnB
Date (2000)	Sep 26 1600{1710 Sep 28 1400{1630	Mar 03 0415{0615
MJD	51813 51815	51606
Flux cal	3C 147	
Phase cal	PKS J0921 2618	
1 RMS	22 Jy/beam	19 Jy/beam
Beam size	28 ⁰ 9 10 ⁰ 40	2 ⁰ 12 2 ⁰ 04
Beam angle	3:98	47:6
V 1974 Cygni (Nova Cygni 1992)		
Band	4.8 GHz (C)	8.4 GHz (X)
Telescope	VLA DnC	VLA CnB
Date (2000)	Jun 27 0800{0945	Mar 09 1500{1600 Mar 10 1330{1430
MJD	51722	51612 51613
Flux cal	3C 286	
Phase cal	Ohio W 538	
1 RMS	24.6 Jy/beam	19.8 Jy/beam
Beam size	13 ⁰ 8 8 ⁰ 03	2 ⁰ 12 0 ⁰ 92
Beam angle	88:9	79:83
RX J0019.8+ 2156 (QR And)		
Band	4.8 GHz (C)	8.4 GHz (X)
Telescope	VLA DnC	VLA CnB
Date (2000)	Jun 27 1300{1530	Mar 11 1810{2050
MJD	51722	51614
Flux cal	3C 48	
Phase cal	PKS J0010+ 1724	
1 RMS	22.7 Jy/beam	19.8 Jy/beam
Beam size	13 ⁰ 3 8 ⁰ 12	2 ⁰ 19 0 ⁰ 95
Beam angle	76:6	88:68
AG Dra		
Band	5.0 GHz (C)	
Telescope	MERLIN	
Date (2000)	Mar 18 1010{1130 Mar 25 0630{2140 Mar 26 0510{2250	
MJD	51621 51628 51629	
Flux cal	3C 286 & OQ 208	
Phase cal	7C 1603+ 6954	
Peak Fluxes	570 Jy	420 Jy
J2000	16 ^h 01 ^m 41 ^s 007	16 ^h 01 ^m 41 ^s 046
J2000	66 48 ⁰ 10 ⁰ 13	66 48 ⁰ 10 ⁰ 46
1 RMS	103 Jy/beam	
Beam size	48.9 68.5 mas	
Beam angle	27:9	

over the VLA we intended to resolve the two unresolved components previously detected, and obtain some information about the source's structure. The MERLIN image has a beam size of 48.9 68.5 mas at an angle of 27:9, and a 1 RMS noise of 103 Jy beam⁻¹ at 4.994 GHz.

The core component is clearly detected in the MERLIN image and is resolved into two point sources at J2000 = 16^h 01^m 41^s007, J2000 = +66 48⁰ 10⁰13 with a flux of 570 Jy (designated as N1 in figure 1(b)), and J2000 = 16^h 01^m 41^s046, J2000 = +66 48⁰ 10⁰46 and a flux of 420 Jy (designated as N2). These fluxes imply a lower limit of 8000 K for the brightness temperature, consistent with the interpretation of the emission being optically thick free-free emission, however, we do not rule out optically thin emission in this paper. We note that the extension to the north of the component N1 is probably due to noise in the image.

The southwest component in the VLA image is not so clearly defined. If the source has not increased in flux between the epochs, and is a point source then it will be indistinguishable from the noise in the MERLIN image (shown in figure 1(c)). We do observe a number of possible point sources with fluxes around 300{350 Jy, but these are ambiguous compared to the noise. We have lowered the contours compared to figure 1(b) to show the noise in more detail.

2.5 New objects

All three VLA fields were imaged with a diameter of 10.2 arcmin in order to check for emission from known sources, and to detect new objects in the fields. However, interferometric images all suffer from bandwidth smearing or chromatic aberration. This is particularly important when the observed bandwidth is large and a wide field is imaged. The effects of these are to smear sources in a radial direction from the phase centre, and to reduce the observed peak flux. The consequence of this effect is that the signal to noise ratio increases with off-axis beam angle.

For an observation taken with a bandwidth of 50 MHz at 8.3 GHz, and with a circular beam 2 arcsec in diameter, a point source will suffer a 10 per cent reduction in flux at a distance of 3 arcmin in 50 arcsec from the phase centre, and a 50 per cent reduction at a distance of around 11 arcmin, this situation becomes more severe with a smaller beam (see Bridle & Schwab (1989) for details).

We have uploaded to the CDS service for Astronomical Catalogues^Y a table which lists the sources taken from the Simbad catalogue together with our limits to the radio emission from the source based on the bandwidth smeared 5 RMS noise. While none of the known sources were detected, we observed 17 new sources with a flux greater than 5 Jy. An uploaded table as above lists these new sources, together with a Gaussian-fitted flux based on the image beam, and true flux due to the bandwidth smearing in the image, (at the bands C and X given in table 1). A spectral index is also calculated from the bandwidth smeared fluxes and follows the convention of S / ν .

We can therefore estimate that the density of sources with flux > 100 Jy is about 200 sources per square degree

^Y <http://cdsweb.u-strasbg.fr/cats/Cats.htm>

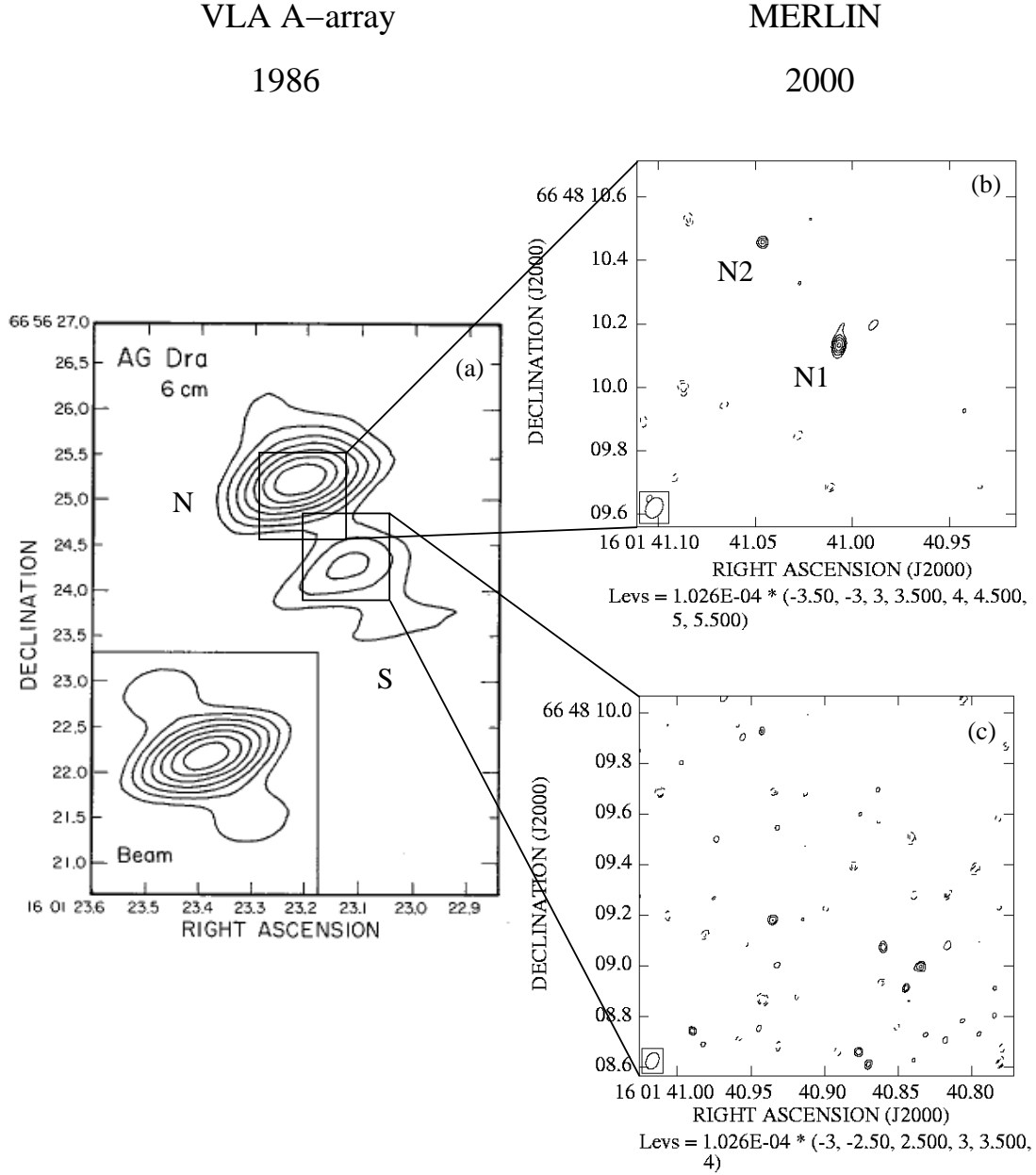


Figure 1. (a) Previous VLA observations of AG Dra. (Torbett & Campbell 1987) (b) Higher resolution MERLIN observations at 4.994 GHz. The core is clearly detected and resolved into two components at the 48.9 μ as resolution (as shown by the beam in the lower left corner). Any extension in component N1 is probably due to noise in the image. Fluxes of components N1 and N2 are 570 and 420 Jy respectively. It is possible that we are resolving out any extended nebula around the core in the MERLIN image. (c) MERLIN observations of the southern VLA component with lower contours to bring out the noise in the image. There are no clear detections of emission.

at 5 GHz, broadly consistent with limits from the deep radio survey by MERLIN of the Hubble Deep Field (Muxlow et al. 1999). The spectral indices of these sources are generally negative or consistent with a negative value, suggesting that most are non-thermal extragalactic objects, however caution has to be drawn to this conclusion since data at the two frequencies is not simultaneous, and there is a difference in angular resolution between the two frequencies.

3 WIND EMISSION

In this section we describe simple analytical models for wind emission and apply them to our sample. Initially we are not interested in where the wind comes from or what it consists of, rather that a generic wind with a particular composition, being ejected at a particular rate from a source at a given distance from us, would produce radio emission. The optically thin flux from a source with these parameters can be calculated and is given by

$$S = 232 \frac{M_{\odot}^{4=3}}{v_{km=s}} g Z^{2-2=3} D^{-2} \text{ Jy} \quad (1)$$

where M_{\odot} is in $M_{\odot} \text{ yr}^{-1}$, μ is the mean atomic weight, $v_{km=s}$ is the wind velocity in km s^{-1} , g is in Hz, Z is the ratio of electron to ion number density, g is the Gaunt factor, Z is the ionic charge and D is the distance in kpc (Wright & Barlow 1975). The Gaunt factor here has a slight dependence on temperature and composition and if one does not consider extremely hot winds, then it can be approximated by

$$g = 9.77 + 1.27 \log_{10} T^{3=2} = Z \quad (2)$$

(Leitherer & Robert 1991).

We can now investigate in more detail from where the wind originates, what is its expected composition and what is the expected radio emission from such a region.

3.1 Generic secondary wind

To create sustained mass transfer between the binary components either the secondary² is undergoing Roche lobe overflow, the wind is providing the accretion via Bondi-Hoyle accretion, or both. Which scenario occurs depends on the nature of the secondary, and the binary parameters.

The symbiotic system AG Dra with a $1.5 M_{\odot}$ K-giant, a $0.5 M_{\odot}$ white dwarf and a period of 544 days does not normally fill its Roche lobe (the stellar radius of the K-giant is $30 R_{\odot}$ and the Roche lobe size is $170 R_{\odot}$). Since the system must be accreting then the logical conclusion is that the secondary is on the Asymptotic Giant Branch (AGB) and feeding the primary by a slow, dense wind. Out of the four sources considered here, this is the most likely to be feeding its environment directly by a wind. Calculating the expected flux from this wind uses a temperature, velocity, outflow and distance of $T = 15000 \text{ K}$, $v = 30 \text{ km s}^{-1}$, $M_{\odot} = 1.2 \{1.7 \cdot 10^{-8} M_{\odot} \text{ yr}^{-1}\}$ and $D = 1.56 \{1.81 \text{ kpc}\}$ from Tomova & Tomov (1999), compositions of $\mu = 1.4$, $Z = 1$ and $Z = 1$ from Nussbaumer & Vogel (1987) and Spergel, Giuliani & Knapp (1983). These parameters yield a flux at 5 GHz of $S_{\nu} = 12 \{26\} \text{ Jy}$.

In contrast to AG Dra, the three other sources either have a small secondary companion and therefore Roche lobe overflow would be providing the mass-transfer, or as in the case for V1974 Cyg, radio emission would have faded and dissipated from the time of the last outburst in 1992.

3.2 Evaporated secondary wind

In the previous section it was shown that only the AGB binary AG Dra would have a strong enough secondary wind to emit significant radio emission. However, if the WD is radiating sufficient soft X-rays then a corona will be formed around the secondary star, which causes a strong stellar wind to be evaporated (Basko & Sunyaev 1973). This type of interaction has been investigated in the context of the supersoft sources by van Teeseling & King (1998, hereafter vTK 98)

² In this paper we use the convention that the WD is designated the primary object and the companion, or donor, is designated the secondary. Subscripts 1 and 2 are used in mass and radius relationships to distinguish between these two objects

and they show that the mass loss rate in the secondary due to irradiation is

$$\dot{M}_{-7} \approx 3 \frac{r_2}{a_9} (m_2 L_{30})^{1=2} M_{\odot} \text{ yr}^{-1} \quad (3)$$

where ϵ is an irradiation efficiency factor, r_2 is the radius of the secondary in solar units, a_9 is orbital separation in units of 10^9 m , m_2 is the mass of the secondary in solar units, L_{30} is the irradiation luminosity in units of 10^{30} J s^{-1} ($10^{37} \text{ erg s}^{-1}$), ϵ is an ionisation efficiency parameter, and \dot{M}_{-7} is given in units of 10^{-7} . It is reasonable, therefore, to assume that since the supersoft sources produce soft X-rays during quiescence from their sustained nuclear burning, that the majority (if not all) of the supersoft sources have mass losses which are wind dominated.

To obtain an estimate for the mass loss from the secondary due to irradiation from the WD, some assumptions to the geometry of the system need to be made. In equation 3, the variable ϵ is an efficiency parameter representing the fraction of the companion's face which is being radiated and the fraction of the wind mass escaping the system. Commentary on the importance of ϵ is given in Knigge, King & Patterson (2000), and a value of 1 is expected. The other unknown parameter in equation 3 is the efficiency of the incident radiation in driving a wind, ϵ . For a wide range of temperatures, including the expected temperature of the irradiation (few 10^5 K), $\epsilon \approx 1$. We can therefore calculate an estimation for the mass-loss in the wind from the secondary, which is given in table 2.

Together with the mass-loss rate and equation 1, the flux from the wind can be found. Unfortunately, the expected fluxes are not as precise as one hopes as a large number of important parameters such as composition (μ , Z), wind temperature and velocity (T and v_1) are unknown.

van Teeseling & King (1998) consider He II to be the main absorber of the WD radiation, which has implications to the composition and temperature of the resulting wind. The temperature of the wind will range from the ionisation temperature of He II to the temperature of the incident radiation, so we use a wind temperature of $T \approx 5 \cdot 10^5$ in this paper. The composition of a purely He II wind would give values for the mean atomic weight ($\mu = 4$), the electron to ion number density ratio ($Z = 2$) and the ionic charge ($Z = 2$). It would be surprising if these were realistic values for the wind, but they are useful approximations and only enter the wind-flux equation (1) as $S \propto \mu^{4=3} Z^{2=3} Z^{4=3}$ and so, small changes would not have a large effect on the estimation. The final variable to estimate is the wind velocity, v_1 . vTK 98 approximate the velocity to be 0.3 times the isothermal sound speed. For sound speeds of the order 100 km s^{-1} this would give approximate wind velocities of 30 km s^{-1} . Using these approximations to the wind gives flux estimates at 5 GHz (S_C) and 8.3 GHz (S_X) shown in Table 2.

3.3 White dwarf wind

We have tried to estimate the radio flux from a white dwarf wind, but the uncertainties are too large to confidently quote numbers. Both Bondi-Hoyle and Roche lobe overflow accretion cannot be reliably used to predict the mass-transfer

Table 2. System parameters and radio fluxes for the supersoft sources.

	RX J0019		AG Dra	V 1974 Cyg	T Pyx
Secondary	F V	M V	K III ^a	M 5 V	M V ^b
Period	15.8 h ^c		554 d ^d	1.95 h ^e	1.8 h ^f
m ₁	0.75 ^g		0.4{0.6 ^d	0.9 0.2 ^h	1.2 ⁱ
m ₂	1.5 ^g	0.31{0.44 ^j	1.5 ^d	0.23 0.08 ⁱ	0.12 ^k
r ₂	1.3	0.36{0.49	28{32 ^d	0.27 0.08	0.17 ^l
L ₃₀	0.3{0.9 ^m		0.14 ⁿ	2 ^o	0.2 ^p
a ₉	2.9	1.79{1.87	249	0.57 0.04	0.57
M ₋₇	1.3	0.18{0.52	0.17	1.0 0.5	0.14
D (kpc)	2.1 ^m		1.7 0.1 ^a	1.8 ^q	3.5 1.0 ^p
T	5 10 ^{5 r}		5 10 ^{5 r}	5 10 ^{5 r}	5 10 ^{5 r}
V _{km=s}	60		60	60	60
R _C (R _⊙)	510	140{280	130	430 150	120
R _X (R _⊙)	360	95{190	90	300 110	80
S _C (theoretical secondary) (Jy)			12{26		
S _C (theoretical evaporated) (Jy)	110	7.5{31	11	110 70	2.6 1.4
S _X (theoretical evaporated) (Jy)	140	10{43	15	160 100	3.5 1.9
S _C (observed) (Jy)	< 100		1000	< 120	< 110
S _X (observed) (Jy)	< 80		{	< 100	< 95

^a Tomov, Tomova & Ivanova (2000)^b Szkody & Feinswog (1988)^c Will & Barwig (1996)^d Mikolajewska et al. (1995)^e Skillman et al. (1997)^f Schaefer et al. (1992)^g Meyer-Hofmeister, Schandl & Meyer (1997)^h Retter, Leibowitz & Ofek (1997)ⁱ Contini & Prialnik (1997)^j Deufelet et al. (1999)^k Clemens et al. (1998); Patterson (1998)^l Paczynski (1971)^m Beuermann et al. (1995)ⁿ Greiner et al. (2000)^o Kahabka & van den Heuvel (1997)^p Patterson et al. (1998)^q Chocholet et al. (1993); Rosino et al. (1996)^r van Teeseling & King (1998)

rate, and therefore the amount of excess material that the white dwarf can process is also undetermined.

3.4 Observational comments to wind emission

From our MERLIN and VLA observations we can provide the flux for AG Draconis and upper limits to the fluxes of the other three supersoft sources in this paper (presented in table 2). Given the spread in the observable system parameters, the expected flux for all three non-detected sources is at, or below the 5 σ cutoff for detections. The surprise in this analysis is with AG Dra where we detect with MERLIN two unresolved point sources with a combined flux of 1 mJy. This is much larger than both the wind flux and an evaporated wind at that frequency of around 10–20 Jy and so we can conclude either the assumptions used in these models are unrealistic, or a different emission mechanism is producing the observed radio flux.

It could be significant that the only detected fluxes originate from a K giant secondary rather than F or M dwarfs. The geometry and accretion in AG Dra is not expected to

be from Roche lobe overflow, but rather from the wind of the AGB secondary.

4 CONCLUSIONS

We have searched for quiescent, persistent radio emission from the northern hemisphere supersoft X-ray sources, and taken a high resolution image of the one known source with emission.

We have improved the radio positions, source size and flux from the persistent emitter AG Dra with MERLIN. The core is resolved at the milliarcsec scale into two components with a combined flux of 1000 Jy. It is possible that the core detected in the VLA image has significant nebulosity and is resolved out by the higher MERLIN resolution. A possible south component detected by the VLA was unconfirmed, although this could be due to it having a flux lower than the noise in the MERLIN image, or also being resolved out.

No new emission was detected from RX J0019.8+2156, T Pyx and V 1974 Cygni down to a 1 RMS noise level of

around 20 Jy beam⁻¹. No emission was detected from any previously known Galactic or extragalactic source in the 3, 104 square arcsec fields imaged, and we place upper limits to radio emission from these sources.

We have investigated possible causes of radio emission from a wind environment, both directly from the secondary star, and also as a consequence of the high X-ray luminosity from the WD.

A total of 17 new point-sources were imaged with fluxes between 100 and 1500 Jy giving an estimate to the density of sources with a flux > 100 Jy of 200 per square degree, at 5 GHz, in this region of the sky.

5 ACKNOWLEDGMENTS

RNO wishes to thank the hospitality of the MERLIN national facility at the Jodrell Bank Observatory, especially Tom Muxlow. SC acknowledges support from grant F/00-180/A from the Leverhulme Trust.

The National Radio Astronomy Observatory is a facility of the National Science Foundation operated under cooperative agreement by Associated Universities, Inc. MERLIN is a national facility operated by the University of Manchester on behalf of PPARC. This research has made use of the SIMBAD database, operated at CDS, Strasbourg, France

REFERENCES

- Basko M M., Sunyaev R A., 1973, *ApSS*, 23, 117
- Becker C M., Remillard R A., Rappaport S A., McCintock J E., 1998, *ApJ*, 506, 880
- Beuermann K., et al., 1995, *A & A*, 280, L9
- Bridle A H., Schwab F R., 1989, 'Wide-field imaging I: Bandwidth and time-average smearing', Lecture 13 in *Synthesis Imaging in Radio Astronomy*, *ASP Conference Series*, 6, 247
- Chochol D., Hric L., Urban Z., Koszka R., Grygar J., Papoušek J., 1993, *A & A*, 277, 103
- Clemens J C., Reid I N., Gizis J E., O'Brien M S., 1998, *ApJ*, 496, 352
- Contini M., Prialnik D., 1997, *ApJ*, 475, 803
- Cowley A P., Schmittke P C., Hutchings J B., Crampton D., McGath T K., 1993, *ApJ*, 418, L63
- Deufel B., Barwig H., Simic D., Wolf S., Dorry N., 1999, *A & A*, 343, 455
- Duerbeck W H., Sitter W C., 1987, *Ap & SS*, 131, 467
- Eyres S P., Davis R J., Bode M P., 1996, *MNRAS*, 279, 249
- Fender R P., Southwell K., Tzioumis A K., 1998, *MNRAS*, 298, 692
- Greiner J., 2000, *New Astr.*, 5, 137
- Hjellming R M., 1992, *IAUC* 5502
- Kahabka P., van den Heuvel E P J., 1997, *ARA & A*, 35, 69
- Knigge Ch., King A R., Patterson J., 2000, *A & A*, 364, L75
- Leavitt H., 1914, *Astron. Nachr.*, 197, 407
- Leitherer C., Robert C., 1991, *ApJ*, 377, 629
- Margon B., Deutsch E W., 1998, *ApJ*, 498, L61
- Meyer-Hofmeister E., Schandl S., Meyer F., 1997, *A & A*, 321, 245
- Michałowska J., Kenyon S J., Michałowski M., Garcia M R., 1996, *AJ*, 109, 1289
- Motch C., 1998, *A & A*, 338, L13
- Muxlow T W B., Wilkinson P N., Richards A M S., Kellermann K I., Richards E A., Garrett M A., 1999, *New AR*, 43, 623
- Nussbaumer H., Vogel M., 1987, *A & A*, 182, 51
- O'Brien T J., Cohen J G., 1998, *ApJ*, 498, L59
- Paczynski B., 1971, *ARA & A*, 9, 183
- Pakull M W., Moche C., Bianchi L., Thomas H C., Guibert J., Beaulieu J P., Grison P., Schaeidt S., 1993, *A & A*, 278, L39
- Patterson J., 1998, *PASP*, 110, 1132
- Patterson J. et al., 1998, *PASP*, 110, 380
- Quaintrell H., Fender R P., 1998, *A & A*, 335, 17
- Retter A., Leibowitz E M., Ofe E O., 1997, *MNRAS*, 286, 745
- Rosino L., Iijima T., Rafanelli P., Radovich M., Esenoglu H., Della Valle M., 1996, *A & A*, 315, 463
- Schaefer B E., Landolt A J., Vogt N., Buckley D., Warner B., Walker A R., Bond H E., 1992, *ApJS*, 81, 321
- Schaeidt S., Hasinger G., Trumper J., 1993, *A & A*, 270, L9
- Sequist E R., Krolec M., Taylor A R., 1993, *ApJ*, 410, 260
- Shahbaz T., Livio M., Southwell K A., Charles P A., 1997, *ApJ*, 484, L39
- Shara M M., Zurek D R., Williams R E., Prialnik D., Gilmozzi R., Motz F J., 1997, *AJ*, 114, 258
- Skillman D R., Harvey D., Patterson J., Vanmunster T., 1997, *PASP*, 109, 114
- Southwell K A., Livio M., Charles P A., O'Donoghue D., Sutherland W J., 1996, *ApJ*, 470, 1065
- Spergel D N., Giuliani Jr J L., Knapp G R., 1983, *ApJ*, 275, 330
- Szkody P., Feinswogl L., 1988, *ApJ*, 334, 422
- Tomov T., Munari U., Kolev D., Tomasella L., Rejkuba M., 1998, *A & A*, 333, L67
- Tomov N A., Tomova M T., 1999, *A & A*, 347, 151
- Tomov N A., Tomova M T., Ivanova A., 2000, *A & A*, 364, 557
- Torbett M V., Campbell B., 1987, *ApJ*, 318, L29
- van den Heuvel E P J., Battacharya D., Nomoto K., Rappaport S., 1992, *A & A*, 262, 97
- van Teeseling A., King A R., 1998, *A & A*, 338, 957 (vTK 98)
- Will T., Barwig H., 1996, *Workshop on Supersoft X-ray sources*, Garhing, ed J. Greiner, *Lecture Notes in Physics* No 472, Springer Verlag, p. 99
- Williams R E., 1982, *ApJ*, 261, 170
- Wright A E., Barlow M J., 1975, *MNRAS*, 170, 41